Interaction between quantum paraelectricity and ferroelasticity in $SrTiO_3$

2005 J. Phys.: Condens. Matter 17 7009

(http://iopscience.iop.org/0953-8984/17/43/018)

INSTITUTE OF PHYSICS PUBLISHING JOURNAL OF PHYSICS: CONDENSED MATTER

J. Phys.: Condens. Matter **17** (2005) 7009–7022 doi:10.1088/0953-8984/17/43/018

Interaction between quantum paraelectricity and ferroelasticity in $SrTiO_3$

Stuart A Hayward, Finlay D Morrison and James F Scott

Department of Earth Sciences, University of Cambridge, Downing Street, Cambridge CB2 3EQ, UK

E-mail: sah21@esc.cam.ac.uk

Received 4 July 2005, in final form 7 September 2005
Published 14 October 2005
Online at stacks.iop.org/JPhysCM/17/7009

Abstract

The dielectric susceptibility of $SrTiO_3$ is measured as a function of temperature between room temperature and 32 K. These data show an anomaly at approximately 105 K, which is associated with the cubic–tetragonal ferroelastic phase transition. The form of this anomaly is shown to be consistent with biquadratic coupling between the ferroelectric and ferroelastic modes. The quantum paraelectric state of $SrTiO_3$ is studied in the framework of a quantum mechanical Landau potential. The saturation temperature is determined from published measurements of the dielectric susceptibility at very low temperatures. When the coupling to the ferroelastic mode is accounted for, the saturation temperature obtained from these measurements ($\theta_S = 20(1)$ K) is the same as that seen in phase diagrams for the ferroelectric transition, such as T_C versus chemical dopant or O isotope content.

1. Introduction

Quantum paraelectricity occurs when an incipient ferroelectric mode is suppressed by quantum mechanical effects near absolute zero kelvin. This is a special case of the quantum saturation of order parameters [1, 2], where the ferroelectric order parameter fails to become non-zero on cooling, due to the zero-point fluctuations of the order parameter near zero kelvin. Characterizing the crossover from classical to quantum mechanical behaviour provides insights into the soft mode driving the phase transition [3]. Quantum paraelectrics are also useful in cryogenic applications, since the piezoelectric response is enhanced over a wide temperature range in the quantum paraelectric regime [4].

A number of quantum paraelectric systems have been identified, including $KTaO_3$ [5]. However, $SrTiO_3$ is not only the first system in which quantum paraelectricity was identified, but it is also the best-studied system in the current literature. Lemanov [6] and Itoh *et al* [7] review the current state of our experimental knowledge of $SrTiO_3$. Hulm [8] measured the dielectric susceptibility of $SrTiO_3$ as a function of temperature, and found that it increased

strongly on cooling, but became almost independent of temperature below 4.2 K. Barrett [9] found that these results were consistent with the quantum mechanical modification of the Slater mean field theory of the dielectric susceptibility of a ferroelectric material [10].

Several detailed studies of the dielectric behaviour of $SrTiO_3$ have been performed. Müller and Burkhard [11] explicitly introduced the concept of a quantum paraelectric state, and interpreted their results for $0.04\ \mathrm{K} < T < 300\ \mathrm{K}$ using quantum mechanical criticality theory [12]. More recently, Dec and Kleemann [13] have used a modification of the Barrett equation with a nonclassical value of γ to describe the results of their measurements in the temperature range $T < 100$ K.

The other important direction taken by research on quantum paraelectricity in $SrTiO_3$ concerns the effect of various external variables on $SrTiO_3$. Burke and Pressley [14] and Uwe and Sakudo [15] found that application of a [100] uniaxial stress induced ferroelectricity in $SrTiO_3$. Fujii *et al* [16] then determined a phase diagram for the paraelectric–ferroelectric phase transition in (σ, T) space. The stresses induced by structural misfits in epitaxial thin films also allow ferroelectricity to be observed [17, 18]. Micropolar regions in $SrTiO_3$ thin films have been observed [19], probably associated with oxygen vacancies.

The effects of various chemical substitutions on the ferroelectric transition have been studied. Ca-doped $SrTiO_3$ is ferroelectric [20, 21]. Between $SrTiO_3$ and $(Sr_{0.984}Ca_{0.016})TiO_3$, the ferroelectric transition temperature increases with Ca content; however, further increases in Ca content reduce the transition temperature slightly. Lemanov *et al* [22] studied the $Sr_{1-x}Ba_xTiO_3$ system using dielectric spectroscopy and ultrasound experiments to determine the ferroelectric and ferroelastic transition temperatures. Ménoret *et al* [23] studied the structural evolution of the same solid solution by diffraction methods. Guzhva *et al* [24] determined the phase diagrams of the $Sr_{1-x}Cd_xTiO_3$ and $(SrTi)_{1-x}(KNb)_xO_3$ systems.

Itoh *et al* [25, 26] found that replacing ^{16}O with ^{18}O in $SrTiO_3$ also stabilized the ferroelectric phase. The phase diagram for the $SrTi(^{16}O_{1-x}{}^{18}O_x)_3$ system was subsequently determined by Yamanaka *et al* [27]. Furthermore, whilst $SrTi^{18}O_3$ is ferroelectric at ambient pressure, the ferroelectricity vanishes when hydrostatic pressure is applied [28, 29].

Although the physical mechanisms underlying each of these phase diagrams are different, they have remarkably similar phenomenologies. All of the phase diagrams for the paraelectric–ferroelectric phase transition follow the equation $T_C \propto (x - x_0)^{1/2}$, as predicted from theory [12]. This contrasts with the equivalent classical model, $T_C \propto (x - x_0)$. The effect of each of these external variables is to increase the temperature of the paraelectric–ferroelectric transition above the limit where quantum mechanical effects prevent the transition from taking place.

One important, but hitherto unanswered, question is the crystal structure of the ferroelectric phase. Despite the simple crystal structure of the perovskite family of materials, complete crystal structure determination is extremely hard [30]. The symmetry-breaking spontaneous strain due to the phase transition, e_t, is given by

$$e_t = \frac{1}{\sqrt{3}}(2e_3 - e_1 - e_2) = \frac{2}{\sqrt{3}}\left(\frac{c' - a'}{a_0}\right), \tag{1}$$

where c' and a' are the lattice parameters of the tetragonal phase corrected for unit cell doubling, and a_0 is the extrapolated lattice parameter in the absence of the phase transition [31]. Even at 1.5 K, the data in [30] indicate e_t is only 1.5×10^{-3}. Such a small distortion is close to the resolution limit of many diffraction experiments. For this reason, many diffraction studies of $SrTiO_3$ focus on the presence or absence of superlattice reflections, such as those arising from the doubling of the primitive unit cell volume at the $Pm\bar{3}m$–$I4/mcm$ phase transition. Unfortunately, diffraction studies of the ferroelectric phase are even harder. Since ferroelectric

phase transitions do not lead to unit cell doubling, no superlattice reflections are expected; the evidence for a phase transition in the diffraction pattern is (probably very small) splitting of certain diffraction peaks and changes in the intensities of diffraction peaks. Ménoret *et al* [23] studied a number of samples in the $Sr_{1-x}Ba_xTiO_3$ system, but did not observe any peak splitting beyond that found for the $I4/mcm$ structure.

An alternative strategy to determine the structure of the ferroelectric phase is to consider the anisotropy of physical properties, and constrain the point group of the structure on that basis. From the anisotropy of the second harmonic generation signal, Uesu *et al* [32] conclude that the point group of ferroelectric $SrTi^{18}O_3$ is $mm2$. The mechanism of the transition has been studied using NMR spectroscopy by Blinc *et al* [33, 34], who found that Ti in paraelectric $SrTiO_3$ are dynamically disordered, indicating that there is at least a partial order–disorder component to the transition.

The nonclassical behaviours of both the dielectric susceptibility and the various phase diagrams have a common origin in the thermodynamic behaviour of bare $SrTiO_3$, and its response to either an external electrical field or other applied variables. In the mean field limit, such problems are conveniently handled using a quantum mechanical modification of the Landau potential [1, 2]. For a second order phase transition, we have

$$G = \underbrace{\frac{A\theta_S}{2}\left(\coth\left(\frac{\theta_S}{T}\right) - \coth\left(\frac{\theta_S}{T_C}\right)\right)Q^2}_{\text{bare system}} + \underbrace{\frac{B}{4}Q^4 + \frac{Ak\theta_S}{2}xQ^2}_{\text{coupling to external variable}} , \tag{2}$$

where θ_S is a temperature characterizing the crossover from classical to quantum mechanical behaviour, T_C is the *observed* transition temperature, and k is the coupling constant between the order parameter and the external variable (pressure, chemical dopant concentration or suchlike) x. The exact analytical form of equation (2) depends on the dispersion of the relevant soft mode excitation. The simplest model (a dispersionless Einstein oscillator) leads to equation (2). Other dispersion models modify the functional form somewhat, though the numerical values of $G(Q, T, x)$ remain very similar.

For a thermodynamically second order phase transition, the form of the phase diagram follows from the definition that at the transition temperature the Q^2 prefactor changes sign. Using this [35],

$$T_C(x) = \frac{\theta_S}{\coth^{-1}\left(\coth\left(\frac{\theta_S}{T_C^0}\right) - kx\right)}, \tag{3}$$

where T_C^0 is the critical temperature for the system with $x = 0$. Equation (3) was found to describe the (σ, T) phase diagram of $SrTiO_3$ [16] very well, with $\theta_S = 20$ K [35]. Extrapolating the linear part of the (σ, T) phase diagram to $\sigma = 0$ implies that, if the behaviour of $SrTiO_3$ were wholly classical, the ferroelectric transition temperature would be 12 K. Since this is only just above the temperature where the quantum mechanical zero point is reached ($\theta_S/2 = 10$ K), the phase transition to the ferroelectric state is not observed.

Equation (2) is a convenient form of the quantum Landau potential to describe phase transitions which actually occur. However, the description of the quantum paraelectric state (where the phase transition does not occur on cooling to 0 K) is incomplete, since $\coth(\theta_S/T_C)$ can only be in the range $-1 \leqslant \coth(\theta_S/T_C) \leqslant 1$. A more general form of equation (2) (analogous to equation (2) in [36]) is

$$G = \underbrace{\frac{A}{2}\left(\theta_S \coth\left(\frac{\theta_S}{T}\right) - T_B\right)Q^2}_{\text{bare system}} + \frac{B}{4}Q^4 + \underbrace{\frac{Ak\theta_S}{2}xQ^2}_{\substack{\text{coupling to} \\ \text{external variable}}} . \tag{4}$$

From the free energy expression in equation (4), the Barrett equation for the dielectric susceptibility follows by using $\chi^{-1} = \partial^2 G/\partial Q^2$. Setting $x = 0$ and $T > T_C$, we obtain the Barrett equation

$$\chi^{-1} = A\left(\theta_S \coth\left(\frac{\theta_S}{T}\right) - T_B\right), \tag{5}$$

where T_B is the temperature at which the transition *would* happen, *in the absence of quantum mechanical effects*. As with equation (2), minor deviations from equation (4) may exist for different dispersion models. In the classical limit ($T \gg \theta_S$), the Barrett equation [9] simplifies to the Curie–Weiss law:

$$\varepsilon = C/T - T_0. \tag{6}$$

In the classical limit, the Landau critical temperature T_C and the Curie–Weiss temperature T_0 are equivalent. Furthermore, for a second order phase transition, the critical temperature is the temperature at which the phase transition occurs. In the case of a first order transition, the transition temperature (typically labelled T_{TR} in analyses based on Landau theory, but T_C in analyses using the Curie–Weiss law) is somewhat higher than the critical/Curie–Weiss temperature. The appropriate description of the ferroelectric phase transition in normal $SrTiO_3$ is ambiguous, since the phase transition itself does not occur. However, in $SrTi^{18}O_3$, the transition is observed at 24 K. From an absence of thermal hysteresis, Dec *et al* [37] conclude that the transition in $SrTi^{18}O_3$ is second order. Some rounding is seen in the dielectric peak; its most likely origin is slight heterogeneities in the oxygen isotope exchange [38].

Attempts to describe the dielectric behaviour of $SrTiO_3$ using the model described by equations (4) and (5) have been made, but the simple form of the model works very poorly. Müller [39] found that a single fit of the data in [11] was impossible. A fit of data in the range 20 K $< T <$ 300 K works quite well, but the fit does not then describe the behaviour of the dielectric susceptibility at lower temperature. Similarly, a fit to the lower temperature data fails to extrapolate to higher temperatures correctly. Dec and Kleemann [40] modified equation (5) to include a critical exponent γ. The resulting model gave a good fit for $\chi(T)$ data in the range 0 K $< T <$ 120 K. The saturation temperature $\theta_S = 17$ K was similar to the one obtained in [35], but the T_C^0 value (0 K) was different. Furthermore, Dec and Kleemann [40] found that both their critical exponent and the value of θ_S varied quite strongly as a function of Ca doping.

In this study, we aim to reconcile the dielectric data for $SrTiO_3$ with the behaviour of the various phase diagrams in the literature, by defining a single set of quantum saturation parameters which consistently describe both phenomena. In order to do this over a wide temperature interval, and to overcome the difficulties encountered in earlier attempts, we also incorporate the interaction between the ferroelectric and ferroelastic phase transitions in our model of the dielectric susceptibility of the paraelectric phase.

2. Dielectric studies of $SrTiO_3$

2.1. Coupling between the ferroelectric and ferroelastic modes

A full thermodynamic description of the phase transitions in $SrTiO_3$ requires two order parameters: one for the ferroelectric mode which is our main interest here, but also one for the well-known ferroelastic $Pm3m$–$I4/mcm$ phase transition. Although the crystal structure of the ferroelectric phase has not been determined, the symmetry is clearly not the same as that of the ferroelastic phase. As a result, the coupling between the ferroelectric order parameter Q_F and the ferroelastic order parameter Q_T is biquadratic [6, 15, 41], and so the complete free

energy has the form

$$G(Q_F, Q_T) = G(Q_F) + G(Q_T) + \lambda Q_F^2 Q_T^2. \tag{7}$$

The form of the dielectric anomaly following from this free energy expression has been studied by Poon [42], and applied to ammonium hydrogen oxalate hemihydrate. Differentiating equation (6) with respect to Q_F twice, we obtain

$$\chi^{-1} = \frac{\partial^2 G}{\partial Q_F^2} = \frac{d^2 G(Q_F)}{d Q_F^2} + 2\lambda Q_T^2. \tag{8}$$

Equation (8) shows how a ferroelastic phase transition, by its interaction with a ferroelectric instability, can cause a dielectric anomaly. None of the detailed studies of the dielectric behaviour of $SrTiO_3$ in the quantum paraelectric regimes have included this effect explicitly in their analyses. More recent studies of the dielectric susceptibility of $SrTiO_3$ between 90 and 300 K [41, 43, 44] found a deviation from classical Curie–Weiss behaviour at 105–110 K. Viana *et al* [43] made the connection between this anomaly and the ferroelastic phase transition, but argued that the mechanism was the onset and dynamics of ferroelastic twin walls.

The expected forms of χ^{-1} and χ as a function of T, assuming explicit coupling between ferroelastic and ferroelectric order parameters, are shown in figures 1(a) and (b). If λ is taken to be positive, the effect of the ferroelastic phase transition is to reduce the stability of the ferroelectric phase. This is consistent with the results of density-functional calculations [45].

2.2. *Measurements of the dielectric susceptibility of $SrTiO_3$*

Dielectric data were obtained from (100)-oriented $SrTiO_3$ single crystals (Crystal GmbH, Berlin). Data were obtained at 100 kHz using a HP4192A impedance analyser (Hewlett-Packard, Palo Alto, CA) in the temperature range ambient to about 30 K in a closed cycle helium cryostat (model 22C Cryodyne Cryocool, CTI-Cryogenics, Waltham, MA). The cooling rate was approximately 1 K min^{-1}. Electrodes were fabricated from sputtered Au.

Figure 2(a) shows the measured inverse dielectric susceptibility of $SrTiO_3$ as a function of temperature. The data show the expected Curie–Weiss behaviour as indicated by the linear plot. Data fitting in the range 110–300 K give a Curie–Weiss constant, C in equation (6), of $6.23(1) \times 10^4$ K^{-1}, and extrapolated Curie–Weiss temperature, T_0, of 17.0(1) K, in reasonable agreement with those reported previously [11, 46]. Figure 2(b) shows dielectric data in the range 60–140 K. A linear baseline has been determined, using the best fit to the experimental data in the temperature range 110 K $< T <$ 140 K. There is a kink in the ε'^{-1} (T) curve around 100 K, similar to that found before [41, 43, 44] and with a similar form to that predicted for coupling between the ferroelectric and ferroelastic modes (equations (7) and (8)). To investigate this point further, we determined the magnitude of the anomaly in ε'^{-1} as a function of temperature. This is shown in figure 3, together with a curve based on the temperature dependence of the ferroelastic order parameter (based on a range of experimental methods, as reviewed in [47]). There is significant scatter in these results, which will be magnified by the process of determining a small difference between the observed and extrapolated ε'^{-1} values, but these results clearly show that the dielectric susceptibility of $SrTiO_3$ is affected by the interaction with the ferroelastic transition. The dielectric data above 105 K follow classical Curie–Weiss behaviour; fitting data in the range 140–100 K gives the baseline shown in figure 2(b), which gives $T_B = 18(1)$ K. Including the effect of coupling to the octahedral tilting mode reduces the expected T_B to 13(1) K.

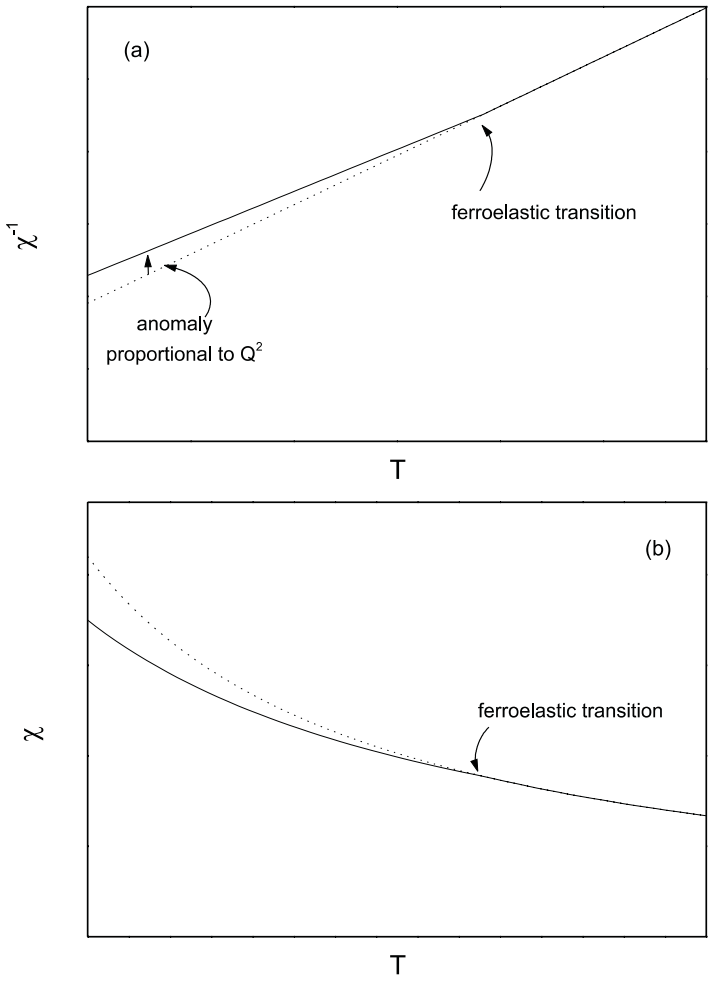

Figure 1. Temperature dependence of (a) inverse dielectric susceptibility and (b) dielectric susceptibility in the vicinity of a coupled ferroelastic phase transition with positive λ. The broken line shows the extrapolated behaviour in the absence of the coupling.

2.3. Application to very low temperature dielectric measurements

Below 105 K, the dielectric susceptibility of $SrTiO_3$ is modified by a contribution from the ferroelastic order parameter. The effect of the ferroelastic phase transition is to enhance the stability of the paraelectric phase. With the coupling strength indicated in figure 2, the classical ferroelectric transition temperature is depressed from 18 to 13 K. This is consistent with the form of the phase diagram for the ferroelastic and ferroelectric transitions in doped $SrTiO_3$ [48]. However, the ferroelastic order parameter is essentially independent of temperature below 30 K [47]. Consequently, dielectric data below this temperature will not have an anomalous form; the effect of the coupling to a constant Q_F^2 term will be a constant shift, relative to the zero-coupling case, in the ferroelectric transition temperature. In figure 4, we show the best fit to the published dielectric susceptibility data [11] in the range $T < 30$ K. In this temperature range, the dielectric susceptibility follows the Barrett equation very well, with $\theta_S = 20(1)$ K. The classical transition temperature obtained from this fit is $T_B = 13(1)$ K.

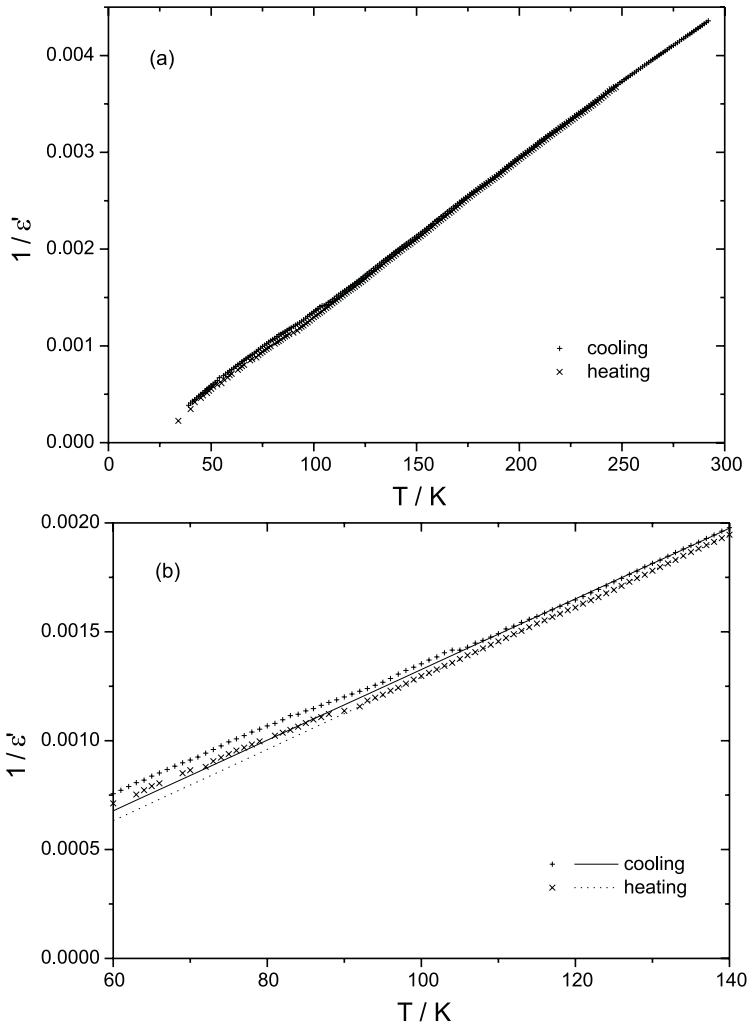

Figure 2. (a) Temperature dependence of the inverse dielectric susceptibility of $SrTiO_3$ between 32 and 293 K. (b) Temperature dependence of the inverse dielectric susceptibility of $SrTiO_3$ between 60 and 140 K. The lines show an extrapolation of the linear fit (classical Curie–Weiss behaviour) to the data for 110 K $< T <$ 140 K. An anomaly is seen below 105 K, associated with the cubic–tetragonal ferroelastic transition.

An important difficulty when fitting dielectric data to the quantum Curie–Weiss law (equation (5)) is the correlation between the fit parameters. The ideal situation is to have an extensive run of high temperature data, as well as measurements in the quantum mechanical range. In the classical limit ($T \gg \theta_S$) the inverse susceptibility of equation (5) is a straight line, allowing a gradient and intercept to be fitted fairly reliably. The quantum mechanical crossover temperature is then unambiguously the temperature at which the linearity breaks down.

Unfortunately, selecting the dielectric data only for the temperature range where the ferroelastic transition is inactive has the effect that the classical behaviour of the ferroelectric transition is not characterized. One solution would be to fit the entire set of dielectric data, but this requires additional fit parameters to characterize the ferroelastic transition and the

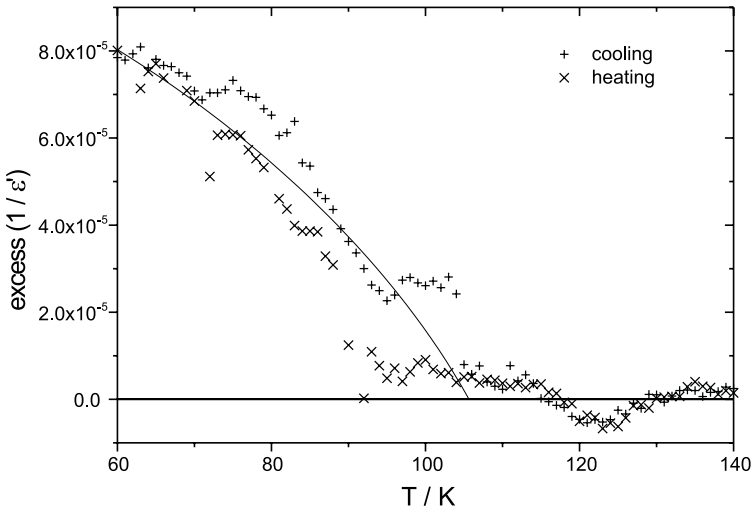

Figure 3. Magnitude of the anomaly in the inverse dielectric susceptibility of $SrTiO_3$ associated with the onset of the $Pm3m$–$I4/mcm$ ferroelastic phase transition. The reference baseline for this excess is a linear fit to $(1/\varepsilon')$ in the temperature range 110 K $< T <$ 140 K. The solid line shows the temperature dependence of Q^2 for the ferroelastic phase transition from [47].

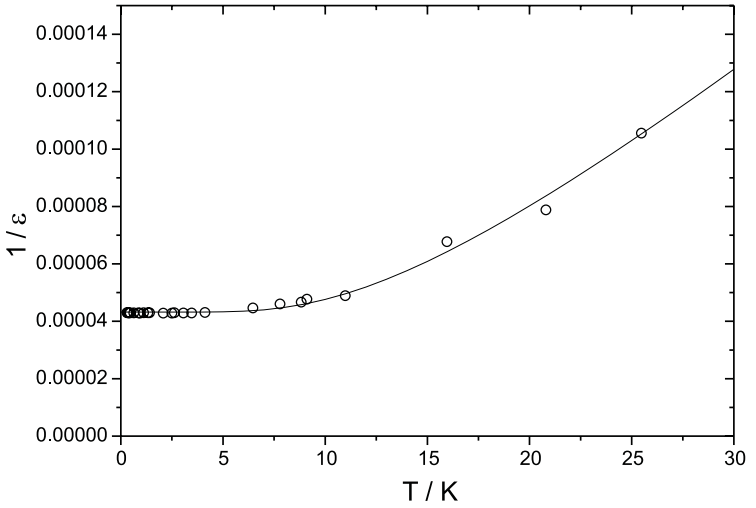

Figure 4. Temperature dependence of the reciprocal of the dielectric susceptibility of $SrTiO_3$, according to the measurements of Müller and Burkhard [11]. The solid line shows a best fit to the Barrett equation, with $\theta_S = 20(1)$ K and $T_B = 13(1)$ K.

interaction between the ferroelectric and ferroelastic transitions. The correlation between T_B and θ_S is positive; if θ_S is underestimated, the effect is to drag the best fit of the classical behaviour to a lower apparent T_B value. Some of the covariance can be mitigated by a judicious choice of fit parameters; equation (5) can be recast as $\chi^{-1} = k\theta_S(\coth(\theta_S/T) - \mu)$. However, even this reformulation cannot solve the underlying problem of an insufficiency of experimental data to fit the model. As a result, the covariances for the fit parameters in the recast model are still extremely large, as shown in the variance–covariance matrix (table 1).

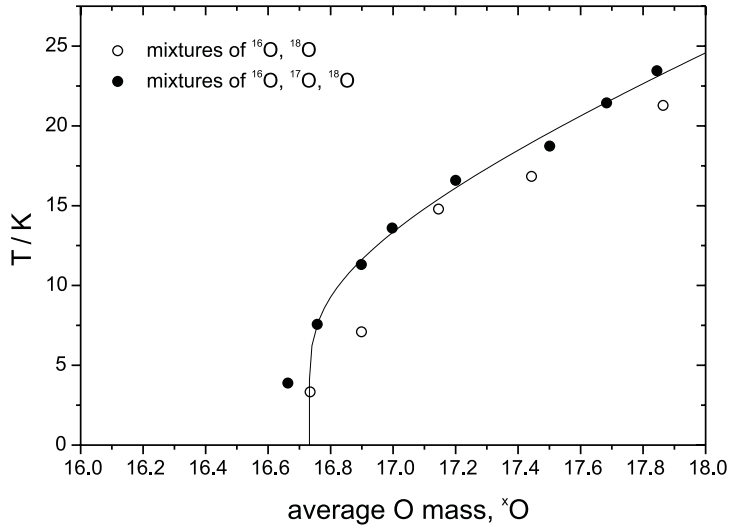

Figure 5. Phase diagram for the ferroelectric phase transition in $SrTiO_3$ as a function of O isotope exchange, using the peak in the dielectric susceptibility to measure the transition temperature. The experimental points are from Itoh and Wang [26, 49].

Table 1. Variance–covariance matrix for Barrett law fit parameters for the dielectric susceptibility of $SrTiO_3$, according to the measurements of Müller and Burkhard [11].

	κ	μ	θ_S (K)
θ_S (K)	0.924	0.967	1
μ	0.982	1	
K	1		

3. Phase diagrams for the ferroelectric–paraelectric phase transition

In an earlier paper [35], we determined the best fit parameters for the paraelectric–ferroelectric phase transition in $SrTiO_3$ as a function of temperature and [100] stress, determined experimentally by Fujii *et al* [16]. Using the model in equation (2), the quantum mechanical saturation temperature $\theta_S = 20(2)$ K and $T_B = 12(2)$ K. We now study some of the other published phase diagrams by the same method.

3.1. Effect of ^{16}O, ^{18}O exchange

Itoh and Wang [49] made mixtures of $SrTi^{16}O_3$, $SrTi^{17}O_3$ and $SrTi^{18}O_3$ to show that the ferroelectric transition temperature depends only on the average isotopic mass of the oxygen in the sample. In figure 5 we fit their results to a quantum Landau model with $\theta_S = 17(3)$ K and $T_B = 9(2)$ K. As with the dielectric data, the lack of higher temperature experimental data causes significant covariance between these two temperatures.

3.2. Effect of $KNbO_3$ doping

Guzhva *et al* [24] found that small amounts of $KNbO_3$ enhanced the ferroelectric transition temperature substantially. In figure 6, the best fit parameters are $\theta_S = 29(10)$ K and

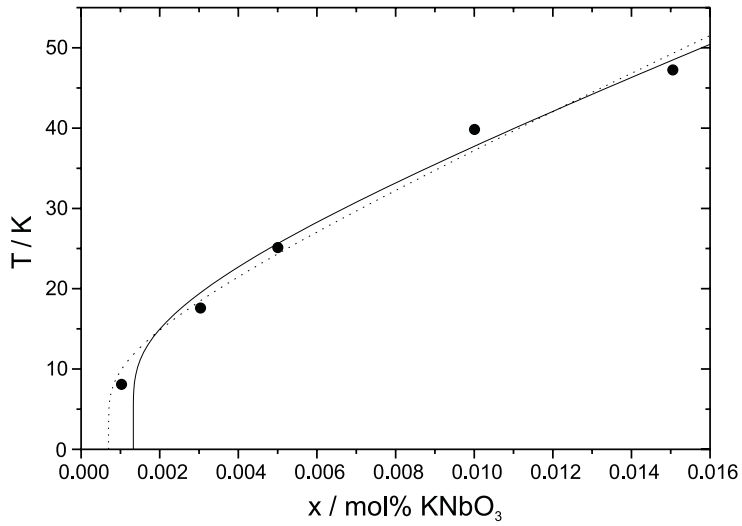

Figure 6. Phase diagram for paraelectric–ferroelectric phase transition in $SrTiO_3$ as a function of $KNbO_3$ doping, using the peak in the dielectric susceptibility to measure the transition temperature. The solid line shows the overall best fit curve. The broken line is a fit with $\theta_S = 20$ K fixed to be consistent with the other results examined here. Experimental data are from Guzhva *et al* [24].

$T_B = 15(5)$ K. The larger errors are due to the relatively small number of data points in the quantum mechanical region. A fit with θ_S fixed at 20 K (leading to $T_B = 11(2)$ K) is only marginally worse, as shown in figure 6. Of course, this is to be expected, given the rather strong covariance between the various parameters, particularly since experimental data within the curved part of the phase diagram are rather sparse.

3.3. Effect of Cd doping

The variation of T_C with Cd doping is more complicated, as studied by Guzhva *et al* [24, 50]. For small dopant concentrations, the behaviour is similar to the other phase diagrams studied here; the available data are not numerous enough to allow all the parameters in equation (2) to be fitted with any reliability, but a fit with $\theta_S = 20$ K is consistent with the data, as shown in figure 7. For samples more Cd rich than $Sr_{0.96}Cd_{0.04}TiO_3$, the transition temperature falls with increasing Cd content, to $Sr_{0.90}Cd_{0.10}TiO_3$. Then, the ferroelectric transition temperature starts to increase again with further Cd doping.

One possible reason for this complexity is the interaction between ferroelectricity and ferroelasticity in the $Sr_{1-x}Cd_xTiO_3$ system. At room temperature, $CdTiO_3$ is orthorhombic $Pbmn$. On heating, $CdTiO_3$ undergoes transitions to structures with space groups $Cmcm$ ($T_C = 493$ K), and $I4/mcm$ ($T_C = 653$ K) [59]. This space group sequence is common in the perovskite family of structures, and is qualitatively similar to the behaviour of the $Sr_{1-x}Ca_xTiO_3$ system, as reviewed in [31]. This similarity is consistent with crystal chemical arguments, since the ionic radii of Shannon [51] for Cd^{2+} (1.33 Å) and Ca^{2+} (1.34 Å) in a 12-coordinated site are so similar, and significantly smaller than Sr^{2+} in the same environment (1.44 Å). Although the (temperature, composition) phase diagram of the $Sr_{1-x}Cd_xTiO_3$ system has not been systematically studied, the most reasonable working hypothesis to explain the observed form of the phase diagram is that the peak in T_C for the ferroelectric phase transition occurs because of a change in symmetry in the paraelectric phase, as shown in figure 7.

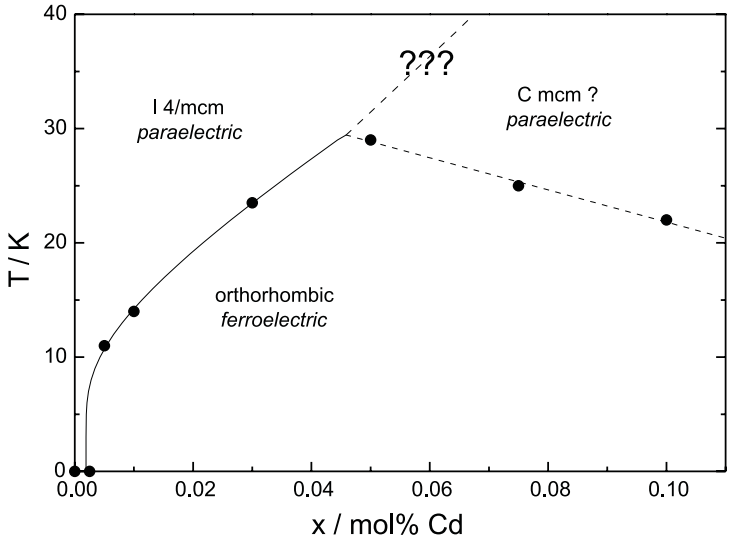

Figure 7. Phase diagram for the $Sr_{1-x}Cd_xTiO_3$ system. The points are measurements of the ferroelectric phase transition temperature using the peak in the dielectric susceptibility by Guzhva *et al* [24, 50]. The solid line fits some of these data to a quantum saturation model with $\theta_S = 20$ K. The broken lines are fits assuming the existence of a tetragonal $\leftrightarrow$ orthorhombic ferroelastic phase transition, which has not yet been observed in this (composition, temperature) range.

4. Discussion

Understanding the behaviour of $SrTiO_3$ requires the consideration of both the ferroelastic instability at 105 K and the ferroelectric instability, which is just inhibited from occurring by zero-point quantum mechanical effects. A long-standing problem in understanding the behaviour of $SrTiO_3$ has been that the dielectric susceptibility fails to follow simple Curie–Weiss behaviour. In this study, we have shown that the non-linearity of ε^{-1} as a function of temperature sets in around 105 K, and has the form expected for coupling between the ferroelectric and ferroelastic order parameters, in a classical (that is, neither quantum mechanical nor critical) model.

The present study does not incorporate several further possible complications to the problem of describing $SrTiO_3$ behaviour below 110 K in a quantitative way. These are mentioned briefly below.

Firstly, the dielectric behaviour of tetragonal $SrTiO_3$ is slightly anisotropic [41], and so the measured dielectric susceptibility will depend on the ferroelastic domain microstructure of the sample. In this study, no specific measures were taken to constrain the sample to be monodomain. In practice, the stress associated with the sputtered electrodes will pole the sample somewhat.

Secondly, there is the question of coupling the ferroelastic, antiferrodistortive (AFE) order parameter near 105 K to defects. In a very detailed study, Höchli and Bruce [52] have shown that the critical exponent describing elastic constants [53, 54] is 1.5(2), in good agreement with that of 3/2 predicted from defect theory [38]. Thus, it might be useful to consider not only the coupling of FE and AFE order parameters, but of the AFE order parameter with polar defects (such as oxygen vacancies). We expect that this will lead just to a renormalization of the coupling between FE and AFE order parameters in the present context.

Thirdly, there is the detailed study of superelasticity in strontium titanate below ca 40 K analysed by Schranz *et al* [55] and Kityk *et al* [56]. This work shows that strain coupling to the ferroelectric order parameter is both strong and complex below 40 K.

Fourthly, we note that antiferroelectric double loops were observed in some samples of single-crystal strontium titanate below ca 62 K by Saifi and Cross [57]. A weak hysteresis was reported as early as 1959 at this temperature [58]. It occurs only after careful annealing and may be due to the resulting stresses induced by the annealing process. Saifi and Cross [57] argue that the energy differences between the various phases of $SrTiO_3$ are extremely small, so that small excess energies from defects or small stresses may play a significant part in changing the equilibrium phase.

By considering only the dielectric data at very low temperatures (where the ferroelastic transition is frozen out), we have obtained a temperature to describe the onset of quantum mechanical effects, $\theta_S = 20$ K. This value is similar to that obtained by Dec and Kleemann [41], but significantly lower than that determined by Müller [40]. Further evidence for the plausibility of $\theta_S = 20$ K comes form direct inspection of the ε^{-1} versus temperature data; the quantum mechanical zero point is reached at $T = \theta_S/2$, and the dielectric susceptibility is essentially independent of temperature below 10 K.

An alternative measure of θ_S comes from phase diagram studies, and we find two striking similarities when comparing these with the dielectric data. Firstly, the saturation temperature appears to have the same value, within experimental error, especially when covariance between the fit parameters is taken into account.

The second point is to consider the notional transition temperature of the ferroelectric transition (in the absence of quantum effects) from the dielectric data. This agrees well with the classical extrapolations of the phase diagrams (T_C versus σ, T_C versus oxygen mass or T_C versus dopant concentration) back to their zero-perturbation cases. In the cases studied here, this extrapolation is problematic, due to the covariance between the various fit parameters, but the classical transition temperature for unperturbed $SrTiO_3$ appears to be around 12 K; this is low enough that the transition is not observed, due to quantum mechanical fluctuations. This observation is consistent with the concept of order parameter coupling, as expressed in Landau potentials like those in equation (2). In this paradigm, the only difference between different applied variables (such as pressure, stress or doping) is the strength of their coupling constants to the order parameter (k in equation (2)).

The role of quantum mechanical fluctuations in inhibiting ferroelectricity in $SrTiO_3$ has long been recognized, and studies of phase diagram behaviour in $SrTiO_3$-based systems have generally used models which incorporate quantum effects. The standard quantum mechanical treatment of this problem leads to the result $T_C(x) \propto (x - x_0)^{1/2}$ [12]. This is consistent with the predictions of the quantum mechanical Landau model, but has the disadvantage that the key parameter x_0 does not have as universal a physical meaning; it is the smallest value of the applied variable which stabilizes the phase transition against quantum mechanical effects. Within a single system (such as $SrTiO_3$) this will be different for different applied variables. By contrast, the quantum mechanical temperature θ_S relates directly to the energy scale of the transition mechanism [2, 3] and should therefore be a constant for a given phase transition.

References

[1] Salje E K H, Wruck B and Marais S C 1991 Order parameter saturation at low temperatures—numerical results for displacive and o/d systems *Ferroelectrics* **124** 185–8

[2] Salje E K H, Wruck B and Thomas H 1991 Order-parameter saturation and low-temperature extension of Landau theory *Z. Phys.* B **82** 399–404

[3] Pérez-Mato J M and Salje E K H 2000 Quantum fluctuations of order parameters in structural phase transitions and the pressure dependence of transition temperatures *J. Phys.: Condens. Matter* **12** L29–34

[4] Grupp D E and Goldman A M 1997 Giant piezoelectric effect in strontium titanate at cryogenic temperatures *Science* **279** 392–4

[5] Rytz D, Höchli U T and Bilz H 1980 Dielectric susceptibility in quantum ferroelectrics *Phys. Rev.* B **22** 359–64

[6] Lemanov V V 2002 Improper ferroelastic $SrTiO_3$ and what we know today about its properties *Ferroelectrics* **265** 1–21

[7] Itoh M, Yagi T, Uesu Y, Kleemann W and Blinc R 2004 Phase transition and random-field induced domain wall response in quantum ferroelectrics $SrTi^{18}O_3$: review and perspective *Sci. Tech. Adv. Mater.* **5** 417–23

[8] Hulm J K 1950 The dielectric properties of some alkaline earth titanates at low temperatures *Proc. Phys. Soc.* A **63** 1184–5

[9] Barrett J H 1952 Dielectric constant in perovskite type crystals *Phys. Rev.* **86** 118–20

[10] Slater J C 1950 The Lorentz correction in barium titanate *Phys. Rev.* **78** 748–61

[11] Müller K A and Burkhard H 1979 $SrTiO_3$: an intrinsic quantum paraelectric below 4 K *Phys. Rev.* B **19** 3593–602

[12] Schneider T, Beck H and Stoll E 1976 Quantum effects in an n-component vector model for structural phase transitions *Phys. Rev.* B **13** 1123–30

[13] Dec J, Kleemann W and Itoh M 2004 Quantum phase transition and dielectric domain wall response of $SrTi^{18}O_3$ *Ferroelectrics* **298** 163–9

[14] Burke W J and Pressley R J 1971 Stress induced ferroelectricity in $SrTiO_3$ *Solid State Commun.* **9** 191–5

[15] Uwe H and Sakudo T 1976 Stress-induced ferroelectricity and soft phonon modes in $SrTiO_3$ *Phys. Rev.* B **13** 271–86

[16] Fujii Y, Uwe H and Sakudo T 1987 Stress-induced quantum ferroelectricity in $SrTiO_3$ *J. Phys. Soc. Japan* **38** 183–9

[17] Pertsev N A, Tagantsev A K and Seter N 2000 Phase transitions and strain-induced ferroelectricity in $SrTiO_3$ epitaxial films *Phys. Rev.* B **61** R825–9

[18] Tikhomirov O, Jiang H and Levy J 2002 Local ferroelectricity in $SrTiO_3$ thin films *Phys. Rev. Lett.* **89** 147601

[19] Sirenko A A, Akimov I A, Fox J R, Clark A M, Li H-C, Si W and Xi X X 1999 Observation of the first-order Raman scattering in $SrTiO_3$ thin films *Phys. Rev. Lett.* **82** 4500–3

[20] Mitsui T and Westphal W B 1961 Dielectric and x-ray studies of $Ca_xBa_{1-x}TiO_3$ and $Ca_xSr_{1-x}TiO_3$ *Phys. Rev.* **124** 1354–9

[21] Bednorz J G and Müller K A 1984 $Sr_{1-x}Ca_xTiO_3$: an XY quantum ferroelectric with transition to randomness *Phys. Rev. Lett.* **52** 2289–92

[22] Lemanov V V, Smirnova E P, Syrnikov P P and Tarakanov E A 1996 Phase transitions and glasslike behaviour in $Sr_{1-x}Ba_xTiO_3$ *Phys. Rev.* B **54** 3151–7

[23] Ménoret C, Kiat J M, Dkhil B, Dunlop M, Dammak H and Hernandez O 2002 Structural evolution and polar order is $Sr_{1-x}Ba_xTiO_3$ *Phys. Rev.* B **65** 224104

[24] Guzhva M E, Lemanov V V, Markovin P A and Shuplygina T A 1998 Ferroelectric behaviour and phase diagrams of $SrTiO_3$-based solid solutions *Ferroelectrics* **218** 93–101

[25] Itoh M, Wang R, Inaguma Y, Yamaguchi T, Shan Y-J and Nakamura T 1999 Ferroelectricity induced by oxygen isotope exchange in strontium titanate *Phys. Rev. Lett.* **82** 3540–3

[26] Itoh M and Wang R P 2000 Quantum ferroelectricity in $SrTiO_3$ induced by oxygen isotope exchange *Appl. Phys. Lett.* **76** 221–3

[27] Yamanka K, Wang R, Itoh M and Ito K 2001 Birefringence study of ferroelectric ordering in oxygen isotope exchanged systems $SrTi(^{16}O_{1-x}{}^{18}O_x)_3$ *J. Phys. Soc. Japan* **70** 3213–6

[28] Wang R, Sakamoto N and Itoh M 2000 Effects of pressure on the dielectric properties of $SrTi^{18}O_3$ and $SrTi^{16}O_3$ single crystals *Phys. Rev.* B **62** R3577–80

[29] Venturini E L, Samara G A, Itoh M and Wang R 2004 Pressure as a probe of the physics of ^{18}O-substituted $SrTiO_3$ *Phys. Rev.* B **69** 184105

[30] Kiat J M and Roisnel T 1996 Rietveld analysis of strontium titanate in the Müller state *J. Phys.: Condens. Matter* **8** 3471–5

[31] Carpenter M A, Becerro A I and Seifert F 2001 Strain analysis of phase transitions in (Ca, Sr)TiO_3 perovskites *Am. Mineral.* **86** 348–63

[32] Uesu Y, Naki R, Kato N, Menoret C, Kiat J-M, Itoh M, Narahashi M and Kyomen T 2003 SHG microscopic studies on low temperature phase transitions of $SrTi^{16}O_3$ and $SrTi^{18}O_3$ *Ferroelectrics* **285** 19–26

[33] Blinc R, Zalar B, Lebar A and Itoh M 2003 Disorder in $BaTiO_3$ and $SrTiO_3$ and the 'ferroelectric' transition in $SrTi^{18}O_3$ *Fundamental Physics of Ferroelectrics 2003* ed P K Davies and D J Singh (Melville, NY: American Institute of Physics) pp 20–5

[34] Blinc R, Zalar B, Laguta V V and Itoh M 2005 Order–disorder component in the phase transition mechanism of ^{18}O enriched strontium titanate *Phys. Rev. Lett.* **94** 147601

[35] Hayward S A and Salje E K H 1998 Low temperature phase diagrams: non-linearities due to the quantum mechanical saturation of order parameters *J. Phys.: Condens. Matter* **10** 1421–30
[36] Prosandeev S A, Kleemann W, Westwański B and Dec J 1999 Quantum paraelectricity in the mean-field approximation *Phys. Rev.* B **60** 14489–91
[37] Dec J, Kleemann W and Itoh M 2004 Quantum phase transition and dielectric domain wall response of $SrTi^{18}O_3$ *Ferroelectrics* **298** 163–9
[38] Levanyuk A P and Sigov A S 1988 *Defects and Structural Phase Transitions* (New York: Gordon and Breach)
[39] Müller K A 1985 Quantum para-, ferro- and random electric behaviors in oxide perovskites *Japan. J. Appl. Phys.* **24** (Suppl. 24-2) 89–93
[40] Dec J and Kleemann W 1998 From Barrett to generalised quantum Curie–Weiss Law *Solid State Commun.* **106** 695–9
[41] Sakudo Y and Unoki H 1971 Dielectric properties of $SrTiO_3$ at low temperatures *Phys. Rev. Lett.* **26** 851–3
[42] Poon W C K 1991 Order parameter coupling and dielectric anomaly in ammonium hydrogen oxalate hemihydrate *J. Phys.: Condens. Matter* **3** 1207–10
[43] Viana R, Lunkenheimer P, Hemberger J, Böhmer R and Loidl A 1994 Dielectric spectroscopy in $SrTiO_3$ *Phys. Rev.* B **50** 601–4
[44] Trainer M 2001 Ferroelectricity: measurement of the dielectric susceptibility of strontium titanate at low temperatures *Am. J. Phys.* **6** 966–9
[45] Sai N and Vanderbilt D 2000 First-principles study of ferroelectric and antiferrodistortive instabilities in tetragonal $SrTiO_3$ *Phys. Rev.* B **62** 13942–50
[46] Rupprecht G and Bell R O 1964 Dielectric constant in paraelectric perovskites *Phys. Rev.* **135** A748–52
[47] Hayward S A and Salje E K H 1999 Cubic–tetragonal phase transition in $SrTiO_3$ revisited: Landau theory and transition mechanism *Phase Transit.* **68** 501–22
[48] Lemanov V V 1999 Phase transitions in $SrTiO_3$ quantum paraelectric with impurities *Ferroelectrics* **226** 133–46
[49] Itoh M and Wang R P 2003 Universal relation between oxygen mass and T_C in $SrTiO_3$ *J. Phys. Soc. Japan* **72** 1310–1
[50] Guzhva M E, Lemanov V V and Markovin P A 2001 Dielectric studies of phase transitions in the ferroelectric $CdTiO_3$ and the $Sr_{1-x}Cd_xTiO_3$ solid solution *Phys. Solid State* **43** 2146–53
[51] Shannon R D 1976 Revised effective ionic radii and systematic studies of interatomic distances in halides and chalcogenides *Acta Crystallogr.* A **32** 751–67
[52] Höchli U T and Bruce A D 1980 Elastic critical behaviour in $SrTiO_3$ *J. Phys. C: Solid State Phys.* **13** 1963–76
[53] Rehwald W 1977 Critical behavior of strontium titanate under stress *Solid State Commun.* **21** 667–70
[54] Bauerle D and Rehwald W 1978 Structural phase transitions in semiconducting strontium titanate *Solid State Commun.* **27** 1343–6
[55] Schranz W, Sondergeld P, Havlik D, Salje E K H, Kityk A V and Scott J F 2000 Low frequency superelasticity and nonlinear elastic behavior of $SrTiO_3$ crystals *Phys. Rev.* B **61** 946–56
[56] Kityk A V, Schranz W, Sondergeld P, Havlik D, Salje E K H and Scott J F 2000 Nonlinear elastic behavior of $SrTiO_3$ crystals in the quantum paraelectric regime *Europhys. Lett.* **50** 41–7
[57] Saifi M A and Cross L E 1970 Dielectric properties of $SrTiO_3$ at low temperatures *Phys. Rev.* B **2** 677–84
[58] Weaver H E 1959 Dielectric properties of single-crystal $SrTiO_3$ at low temperatures *J. Phys. Chem. Solids* **11** 274–9
[59] Kabirov Y V, Kul'buzhev B S and Kupiryanov M F 2001 Structural phase transitions in $CdTiO_3$ *Phys. Solid State* **43** 1968–71